Quantifying damage to coral colonies by waterborne debris during hydrodynamic disturbances

Peter A. David

Quantitative Ecology and Evolution Lab

Department of Biological Sciences

October 10th, 2016

MACQUARIE
University
SYDNEY·AUSTRALIA

Declaration

I wish to acknowledge the following assistance in the research detailed in this report:

Joshua Madin for assistance with experimental analysis. Kyle Zawada for assistance in providing the three-dimensional coral scans. Aaron Harmer and Laura Wilson for assistance with the use of Strand7. Joshua Madin, Rachel Woods and Jessica Thompson for comments on a draft of this manuscript.

All other research described in this report is my own original work and has not been submitted for a higher degree to any other university of institution.

Peter David

10th October 2016

Abstract

Physical bombardment by waterborne debris is a common disturbance in shallow coral reef systems. During hydrodynamic disturbances, such as tropical storms, increases in water velocity elevate drag forces acting on objects—ranging in size from sand to boulders and coral colonies—dislodging and propelling them into nearby coral colonies. Impact by debris can cause a number of injuries, ranging from intra-colony damage (e.g., branch breakage or tissue death) to whole-colony dislodgment. However, the bombardment process is poorly understood, given that it is difficult to observe *in situ* as hydrodynamic disturbances occur. Using 3D coral scans representing five characteristically different growth forms and finite element analysis, I simulated bombardment scenarios by applying increasing point forces to colony meshes. I measured the force required to cause breakage and where that breakage occurred, and found high rates of intra-colony breakage (a mean of 23% across growth forms). There was a significant interaction between colony surface area to volume ratios (SA:V) and the damage outcome (branch breakage or whole-colony dislodgement), but generally the impact force necessary to result in damage decreased as SA:V increased. Traditional models of coral damage during storms only consider hydrodynamic force, however, the results presented here show that bombardment may be the dominant process damaging and killing reef corals during hydrodynamic disturbances.

Key words

Finite element analysis | Bombardment | Cyclone | Coral reef

Introduction

Physical disturbances on coral reefs, such as cyclones, are destructive events and their aftermaths have been well documented. Coral tissue is scoured and damaged, branches are "pruned" and entire colonies are dislodged (Madin 2005; Madin and Connolly 2006; Fabricius et al. 2008; Madin et al. 2014; Puotinen et al. 2016). Partial damage often leads to whole-colony mortality, which can take weeks to unfold (Knowlton et al. 1981). In some cases, colony fragments can reattach to the substrate and resume growth (Smith and Hughes 1999); a considered form of asexual propagation (Tunnicliffe 1981). All in all, the loss of living reef structure is typically dramatic, with cascading consequences for abundances and diversity of reef-associated species, such as the reef fishes (Woodley et al. 1981; Wilson et al. 2006). In spite of this destruction, periodic physical disturbances are believed to be positive for reefs, because they promote species coexistence (Connell 1978) by reducing the dominance by any one species and create space for new corals to recruit.

Despite the importance of physical disturbance in structuring coral reef communities, we have next to no idea what actually occurs during a disturbance event. We cannot directly observe the damage, and so are left to speculate about the processes that led to the resulting bed of rubble. Currently there are two predictive models for coral damage during hydrodynamic disturbances: Massel and Done (1993), which focused on massive corals, and Madin and Connolly (2006), which broadened the focus to all growth forms. However, these traditional models only consider dislodgement via hydrodynamic forces as the damaging process. While there is no doubt that hydrodynamic drag forces are responsible for the dislodgment of whole colonies during an event, less obvious is the damage caused by waterborne debris—much of which is spawned from dislodged colonies themselves. The addition of waterborne debris to models of hydrodynamic disturbance is complicated, because physical bombardment can generate forces greater than drag alone, and any partial colony breakage will reduce drag.

Bombardment is likely to be a ubiquitous process during physical disturbances on reefs. Elevated drag forces act on unattached objects—ranging in size from sand to entire unattached coral colonies—propelling them along the reef and into neighboring colonies. Bombardment is likely to cause severe damage to living corals, ranging from tissue damage and breakage of branches through to the dislodgement of entire colonies. Dislodgement or breakage of colonies at the reef crest will fuel the bombardment process. However, there is a large knowledge gap in the bombardment process, because it is extremely difficult to observe directly. For this reason, there is almost no information as to whether bombardment is an important damage and mortality process during hydrodynamic disturbance nor how if could be modelled.

The aim of my study was to address the knowledge gap of bombardment as an important ecological process during physical disturbances using an engineering modelling approach called finite element analysis (FEA). FEA enabled me to model rates of damage by waterborne debris and contrast these with rates of whole-colony dislodgement for a range of different coral morphologies (=growth forms). My results are preliminary; nevertheless, here I quantify the relative occurrence of breakage versus dislodgement based on growth form and surface area to volume ratios. I hypothesize that an increase of surface area to volume ratio led to an increase in the probability of colony breakage occurring. I then validate that the levels of force required for bombardment to be an important process on reefs that can occur during hydrodynamic disturbances.

Methods

Ten coral colonies were selected from the Natural History Museum coral collection in London that represented five characteristically different growth forms; two of each of branching, digitate, corymbose, plating and massive forms. Three-dimensional (3D) meshes were created for each colony using a CREAFORM EXAScan portable laser scanner (Creaform 2016a) (Figure 1). This system rapidly and precisely scans objects with a resolution of up to 0.2 mm^2 while generating a mesh in real time on a connected computer using the software VXElements (Creaform 2016b). The scanner exposure time was set at 6.00 ms and the accuracy set at 0.5 mm^2.

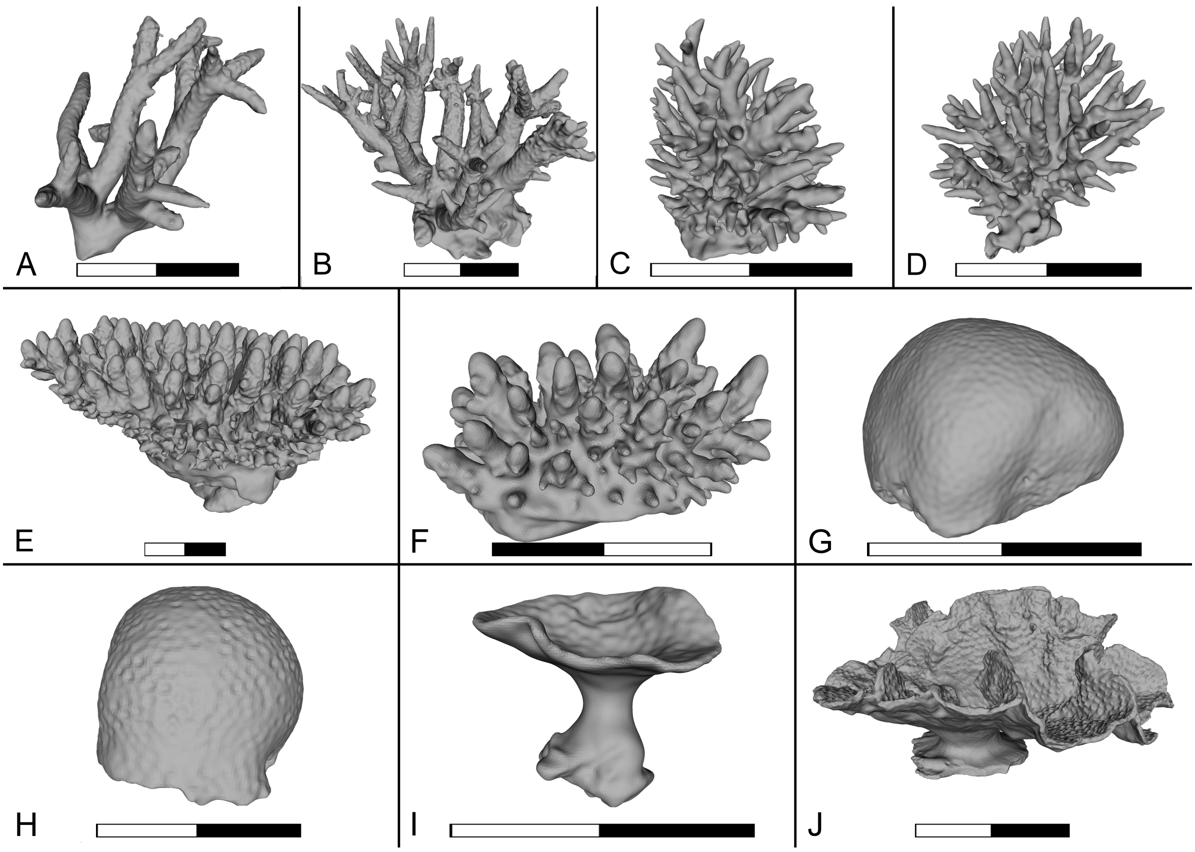

Figure 1. Coral meshes produced by scanning coral colonies with the CREAFORM EXAScan. Growth forms are as follows: Branching; A, B, Corymbose; C, D, Digitate; E, F, Massive; G, H and Plating; I, J. Each black and white scale bar is equal to 10 cm.

Each colony scan was cleaned by first smoothing any obvious surface irregularities, removing non-coral regions (e.g., substrate), and ensuring the mesh was watertight to enable accurate surface area and volume calculations. A mesh-editing program Meshmixer (Autodesk Research 2016) was then used to inspect each of the coral meshes and attach them to a basal block to mimic the reef substrate. Colony surface areas and volumes were calculated using the 'Stability' function in Meshmixer while the basal block was omitted (Table S1). The number of triangles making up each mesh was reduced to fall between 40,000 to 100,000 depending on the complexity of the growth form, which was done to reduce the processing time of FEA while maintaining overall colony shape.

I used Strand7 (Strand7 Pty Ltd 2015) for FEA. In this software meshes were converted to solid meshes. The coral skeleton and reef substrate components were parameterised with elastic moduli, material densities and maximum tensile strengths that were collected from a range of sources, including the Coral Trait Database (Madin et al. 2016) and Madin (2005) (Table 1). All breakage was assumed to occur under tension, because brittle crystalline materials are particularly strong under compression (Madin 2005). In order to mimic how a colony would be impacted by debris, the base of substrate block was restrained from translational and rotational movement and ten bombardment points were randomly selected for each colony mesh. Given processing time constraints, at the time of writing this manuscript each colony was only bombarded from one arbitrarily chosen direction, and material parameters reflect average values (i.e., variation in material properties have not been simulated yet).

Table 1. Growth form and reef substrate material properties

	Branching	Digitate	Corymbose	Plating	Massive	Substrate
Modulus (MPa)	21500	21500	21500	21500	15100	7400
Poissons ratio	0.2	0.2	0.2	0.2	0.2	0.2
Density (g/cm^2)	2.4	2.2	2.2	2.2	1.2	0.8
Breaking point (MPa)	5.01	3.98	3.98	3.98	1.00	0.32

An increasing point load was applied to each bombardment point up until tensile breakage occurred. Breakage rarely occurred at the point the load was applied, and so I measured the point of breakage, and additionally noted if this was intra-colonial (e.g., a branch) or whole colony (e.g., at the basal attachment). Point load increments for each simulation were either 3 MPa for branching, digitate, corymbose and plating growth forms, or 6 MPa for massive growth forms (due to the greater impact force required for breakage or dislodgement). The point of breakage was defined as the point on the colony or substrate where internal tensile stress first exceeded tensile breakage strength of the respective material (substrate or skeleton), which typically occurred lower on a branch or at the colony/substrate interface (Tables S2-11).

In order to assess if the impact forces required to damage colonies were present in the real world, I calculated the forces generated by a range of different massed debris (0.01 – 10 kg) travelling at a range of water velocities (1 – 10 m/s). The maximum water velocity likely to be observed during a cyclone is 5-10 m/s (Madin et al. 2006; Madin et al. 2012). The force generated was estimated according to:

$$F = \frac{2mv}{t}$$

where m is mass of debris, v is velocity of debris, t is the impact period and F is the resulting force generated. I assumed that impact periods are approximately 0.01 seconds based on previous studies of impacts on attached cantilever-like objects (Sun 1977; Ruiz et al. 2000; Mao et al. 2009). Although impact times vary in these studies, the general consensus is that impact times are very short (Youcef-Toumi and Guts 1989; Ma and Chuang 2008), thus this validation figure should be treated as a ball-park estimate.

Data analysis

The outlines of each coral colony were downloaded from Strand7 as xyz coordinate point clouds and an alpha-convex hull (Pateiro-Lopez and Rodriguez-Casal 2016) fitted around the outline in the orientation perpendicular to bombardment. Pairs of impact and breakage points were added to colony outlines and connected with arrows to help visualize the results.

I ran two statistical analyses. First, the probability of breakage (=1) vs. dislodgment (=0) for each bombardment trial was modelled statistically as a function of colony surface area to volume ratio using a binomial generalized linear model (Table 2) in R (R Core Team 2014). Second, impact force required for damage was modelled as a function of surface area to volume ratio and damage outcome type (breakage or dislodgement) using a standard linear model (Table 3). For all analyses, surface area to volume ratios and impact forces were log-transformed, which resulted in the most normally distributed residuals. I tested for an interaction between factors in the second analysis. Analyses were presented as anova tables using the function 'aov' to determine whether one of these factors had a significant effect on the model.

Table 2. Coefficient estimates for the binomial generalized linear model. Null deviance: 21.374 on 8 degrees of freedom, residual deviance: 12.032 on 7 degrees of freedom, AIC: 33.236 and number of Fisher Scoring iterations: 4. Response variable: Probability of breakage vs dislodgement, factors are as follows sa.v: surface area to volume ratio.

	Estimate Std.	Error	t value	p
Intercept	-2.949	0.727	-4.056	>0.001
sa.v	6.133	2.163	2.835	0.005

Table 3. Model estimates table. Residual standard error: 0.2799 on 86 degrees of freedom. Multiple R-squared: 0.5439, Adjusted R-squared: 0.528, F-statistic: 34.19 on 3 and 86 DF, p-value: 1.21e-14. Response variable: log10 impact force, factors are as follows sa.v: surface area to volume ratio and brk.dis: outcome – breakage or dislodgement.

	Estimate Std.	Error	t value	p
Intercept	1.5192	0.2225	6.828	>0.0001
sa.v	-0.1201	0.4313	-0.279	0.7813
brk.dis	-0.4642	0.2401	-1.933	0.0565
sa.v:brk.dis	-0.9812	0.4469	-2.195	0.0308

Results

Across all colonies bombarded, I observed a 77% rate of dislodgement and a 23% rate of intra-colonial breakage (Figure 2). The more complex and upright morphologies (i.e., branching and corymbose) were more likely to suffer branch breakage with a breakage rate of 47%; the plating morphology suffered a breakage rate of 25% with breakage occurring along the plate edges; the more compact digitate morphology suffered a low breakage rate of 10% due to the shorter and robust nature of the branches; and the massive morphology did not display any instances of breakage (Figures 2, S1.1 and S1.2). Overall, there was a significant relationship between the likelihood of breakage and colony surface area to volume ratios, in which colonies with a greater ratio are more likely to break internally than colonies with a smaller ratio (Figure 3).

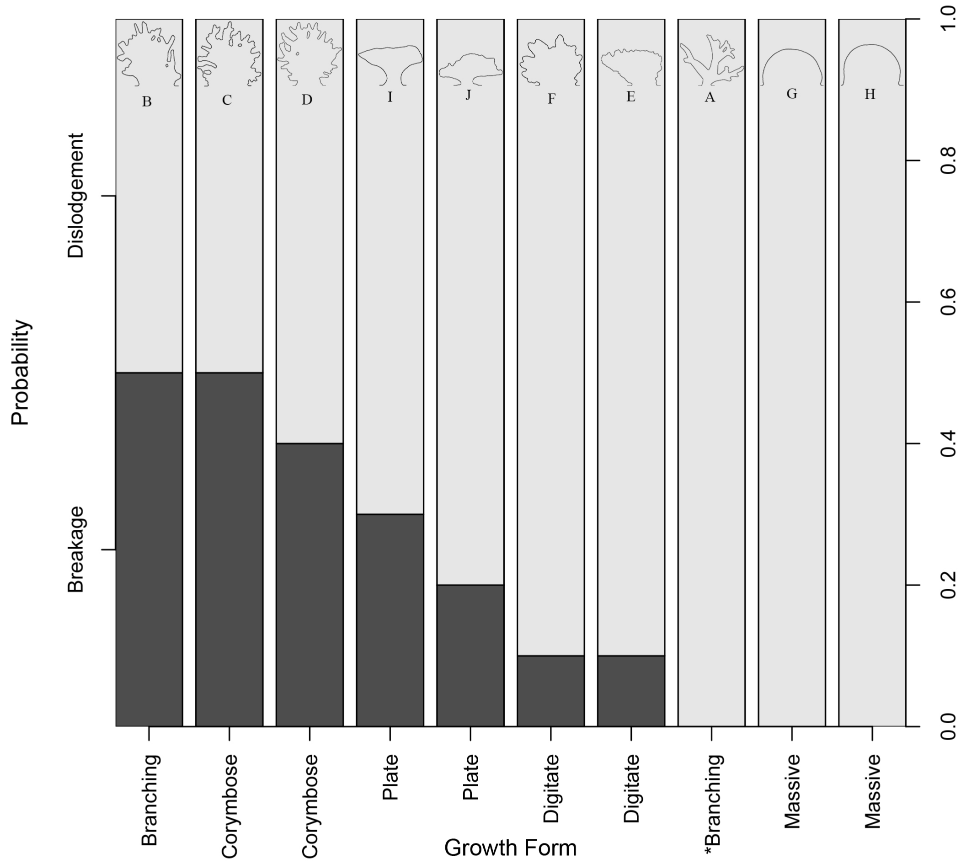

Figure 2. The probability of either breakage or dislodgement for each colony tested. The outline of each colony is projected on the top of each bar. Dark grey: Breakage, light grey: Dislodgement. Each letter below each colony outline corresponds to the same letter and colony in Figure 1. *Removed from analysis due to abnormal results.

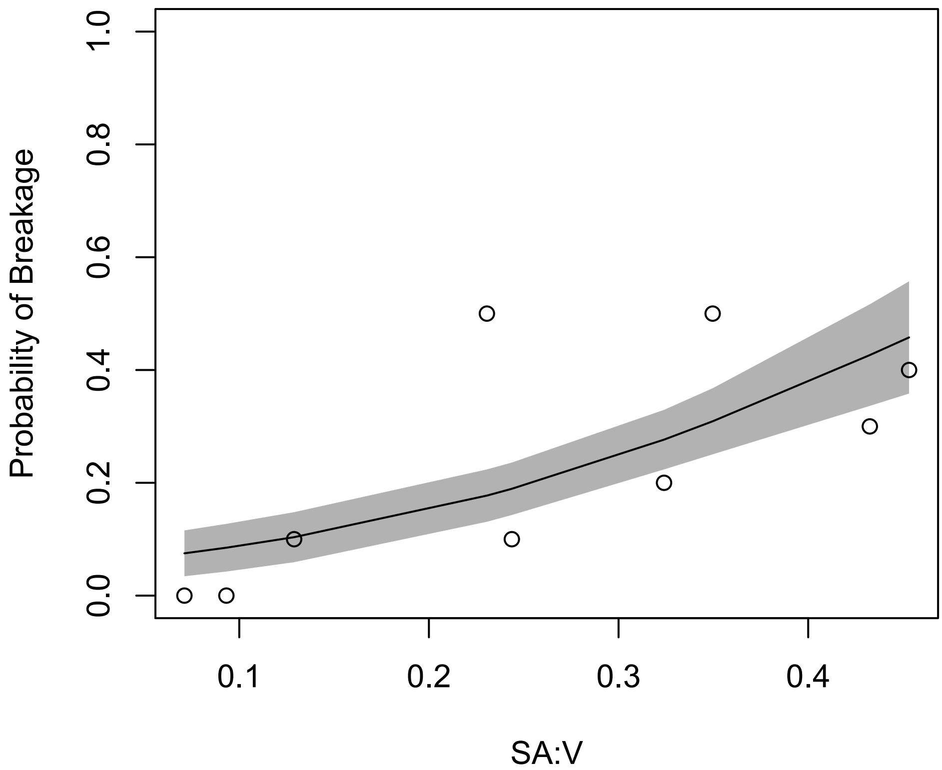

Figure 3. The probability of colony breakage as a function of colony surface area to volume ratio. n=90, confidence bands represent 95%CI.

For the impact forces required to cause damage, I found a significant interaction between colony surface area to volume ratio and the damage outcome type (Df: 1, F: 4.8199, p: 0.03). The impact force necessary for whole colony dislodgement decreases as surface area to volume ratio increases. However, intra-colonial breakage was much less likely to occur in forms with lower surface area to volume ratios; whereas, whether a colony breaks or becomes dislodged becomes indistinguishable at higher surface area to volume ratios (Figure 4). One of the branching growth forms (Figures 1A and S1.1A) was removed for analysis due to abnormal results produced by Strand7, which I suspect was caused by using the mean substrate strength (discussed below). However, it should be noted that removing this sample did not affect the statistical significance of the two analyses, merely strengthened the patterns to a small degree.

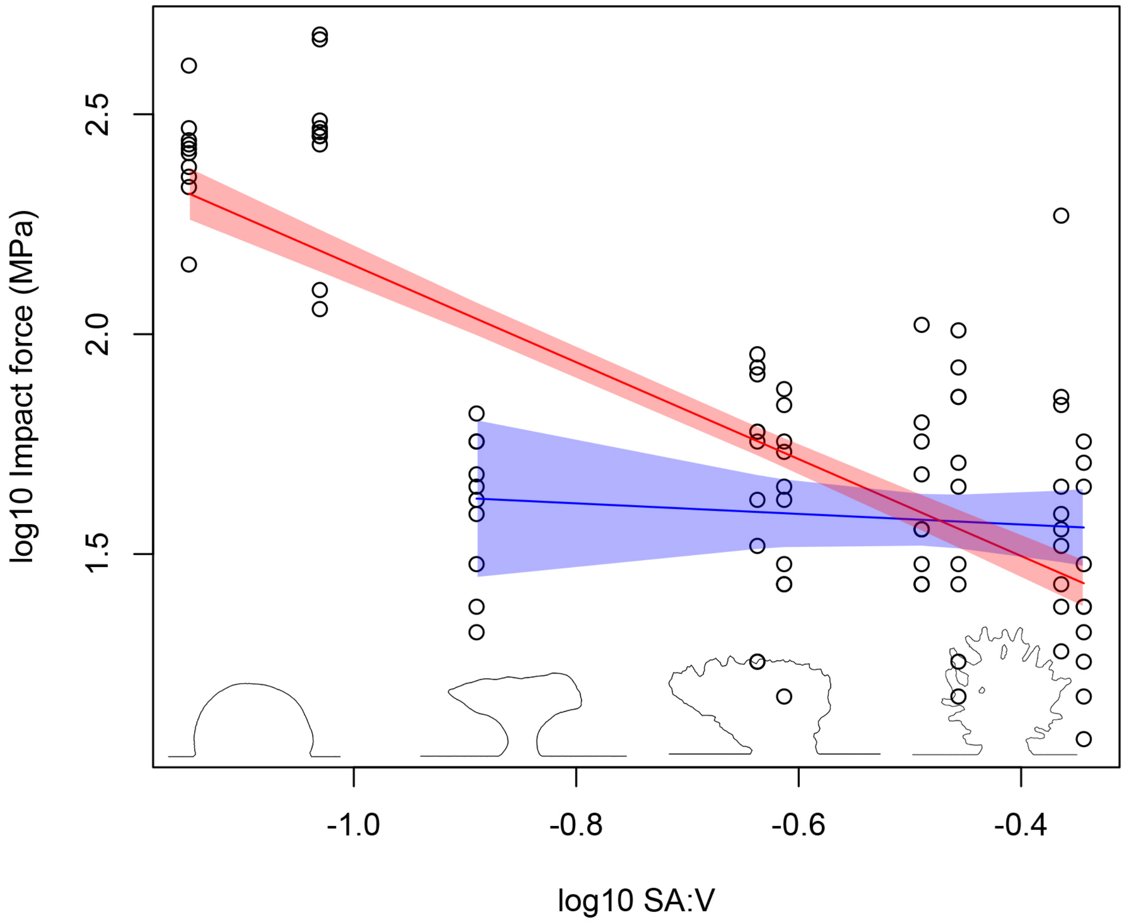

Figure 4. Impact force (log10, MPa) required for breakage or dislodgement as a function of colony surface area to volume ratio (log10, SA:V). The red line and corresponding 95%CI band displays colony dislodgement. The blue line and corresponding 95%CI band displays colony breakage. Coral outlines indicate general shapes that colonies would exhibit corresponding to the SA:V.

Finally, the range of impact forces required to cause damage were all present for the range of projectile velocities and masses likely to be present on a reef during a tropical cyclone (Figure 5).

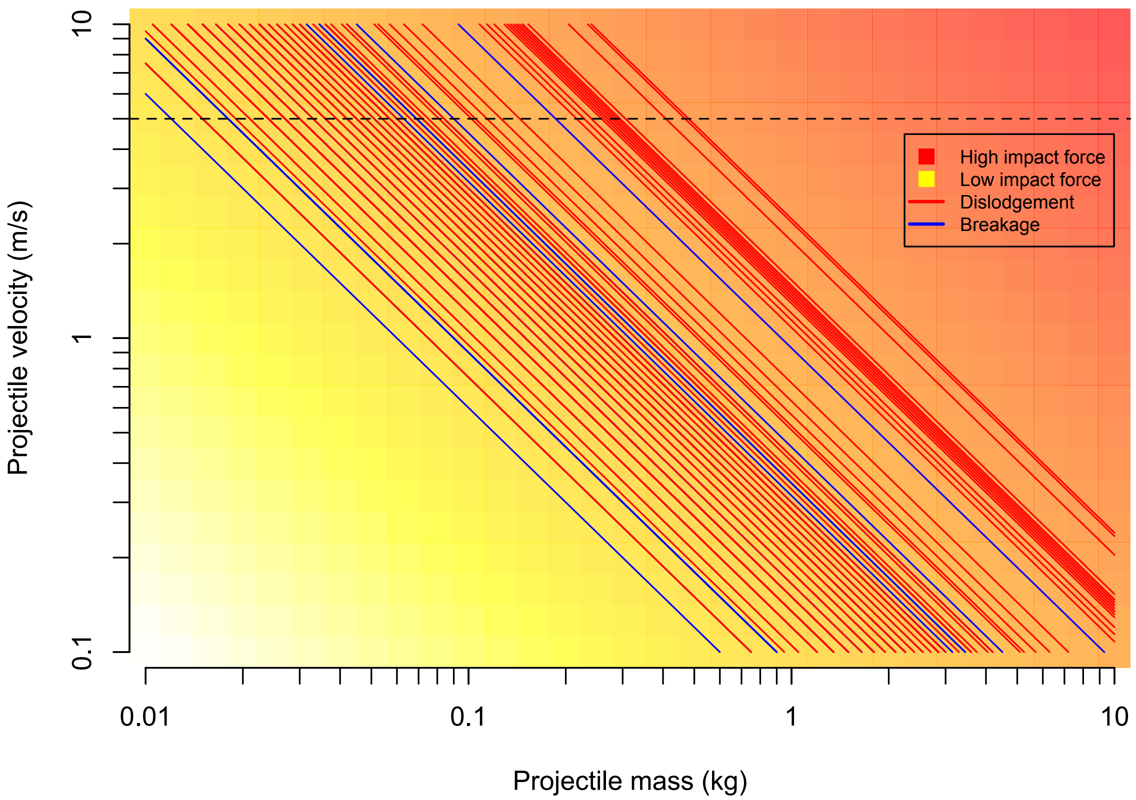

Figure 5. The projectile velocity and mass required to result in a damaging impact (either breakage – blue line, or dislodgement – red line) for each simulation on each growth form. The dashed line represents a projectile velocity of 5 m/s, a speed that would commonly occur over a reef during a cyclone.

Discussion

Whole-colony dislodgement has traditionally been thought to occur before intra-colony breakage in corals, primarily because the tensile strength of reef substrate is much lower than skeletal strength (Madin 2005; Madin and Connolly 2006). This assumption is true when only considering hydrodynamic forces alone, however, my *in situ* observations of a reef following a cyclone, and the analysis presented here, strongly suggests that hydrodynamic dislodgement might be a relatively small part of the story. I found that bombardment causes both colony breakage and whole-colony dislodgement (Figure 2) for the range of projectile masses and water velocities likely to be present during a hydrodynamic disturbance (Figure 5). Furthermore, bombardment caused intra-colonial breakage over 23% of the time on average, which helps explain the high levels of partial mortality observed on reefs following storm events (Woodley et al. 1981) and even tsunamis (Chavanich et al. 2008), particularly for higher SA:V growth forms.

My results suggest that two important considerations need to be made and developed to update current models of storm damage to corals. First, while dislodgement has been shown to be caused through hydrodynamic force (Madin and Connolly 2006), it needs to be considered as a process which can also occur through bombardment. Second, intra-colonial breakage needs to be considered in these models as an important factor that leads to damage as well as to the overall reduction in colony surface area, over which hydrodynamic force and subsequent bombardment act. It is a combination of these factors, which would lead to the most accurate and reliable models of coral colony mechanical vulnerability during physical disturbances.

Further reasoning for revising current mechanical vulnerability models can be seen in the role that the surface area to volume ratio of each colony was shown to have in determining the outcome of a bombardment impact. Surface area to volume ratio is an important trait in determining structural vulnerability of coral colonies, as generally an increase in the surface area to volume ratio corresponds with an increase in the complexity of the colony – the formation of less robust structures such as branches or thin table or plate like constructions. Firstly, as hypothesized, an increase of surface area to volume ratio led to an increase in the probability of colony breakage occurring. Secondly, an increase in surface area to volume ratio also led to significant decrease in the amount of force required to cause colony dislodgement and a slight decrease in the amount of force required to cause colony breakage. Thus these two results are of utmost interest in determining the mechanical vulnerability of coral colonies. Current models look at coral size as a factor in determining mechanical vulnerability. These models have shown that generally, for growth forms other than massive, as colony size increases so does the colony shape factor (CSF), a measurement of mechanical vulnerability (Madin and Connolly 2006; Madin et al. 2014). However, with my data indicating the surface area to volume ratio plays a vital role in determining mechanical vulnerability, it would be logical to integrate this relationship into current CSF models. This would allow for more accurate predictions of vulnerability measures that not only include dislodgement as a factor but branch breakage as well.

Furthermore, another potential reason to revise current mechanical vulnerability models can be seen in the water velocity results displayed in figure 5. These results may indicate that when waterborne debris is present there is a lower threshold for water velocity that might be considered dangerous for corals when compared to those previously shown in hydrodynamic-only predictions of damage (Madin and Connolly 2006; Madin et al. 2006). While these results are only preliminary, it may indicate that current models could hypothetically be underestimating damage resulting from minor storms, which display lowered water velocities.

There are a wide range of ecological effects on colonies themselves as a result of colony breakage (branch pruning). One of the most common results of branch loss is exposed tissue becoming diseased. It is very well documented that injured coral tissue such as that caused by branch breakage is likely to increase the appearance of, and susceptibility to, disease (Hawkins and Roberts 1992; Winkler et al. 2004; Guillemot et al. 2010; Brandt et al. 2013; Katz et al. 2014), as well as increasing the colonies susceptibility to predation (Henry and

Hart 2005; Guillemot et al. 2010). Furthermore, Henry and Hart (2005) have shown when colonies are able to begin to recover injury, they display reduced functions of growth, sexual reproduction and competition. This reduced function of injured corals is undoubtedly linked to the increased energetic costs of recovery and the cost of attempting to resist potential disease. Though in contrast it is thought that in some cases the lower coral cover associated with the aftermath of a cyclone may be beneficial in resisting disease. Bruno et al. (2007) suggests that for the case of white syndrome coral cover must be high in order for outbreaks to occur, and cover is unlikely to be high after a hydrodynamic disturbance. Sub-lethal effects that corals suffer after a disturbance event are highly likely to lead to delayed mortality (Knowlton et al. 1981). In cases that do not lead to eventual mortality, these colonies are likely to be severely affected by the increasing occurrence and potency of other disturbances such as the most recent bleaching event described on the Great Barrier Reef (Hughes 2016).

Effects of hydrodynamic disturbances may also have positive outcomes for some colonies which suffer breakage. In some cases, fragments broken off certain corals such as *Acropora* species are able to re-fuse to the substrate or other colonies and survive (Highsmith 1982; Wallace 1985; Smith and Hughes 1999; Lirman 2000). Not only does this form of asexual propagation (Tunnicliffe 1981) have potential to add material to reefs for growth and it also allows species extend their local distribution. Though it has also been suggested that the benefits of asexual propagation are offset by the negative effects of cyclones, that can lead to the death of fragments through scouring, sedimentation, the turning over of the coral fragments and disease (Bak and Criens 1981; Cooke and Marx 2015).

While colony branch breakage has a range of ecological effects on colonies themselves, it also plays a vital role for several ecosystem functions. Branch breakage can lead to significant reductions in habitat complexity, as vulnerable growth forms which are key in maintaining complexity are easily pruned (Guillemot et al. 2010). It is these complex yet vulnerable growth forms which in turn drive valuable ecosystem functions for assemblages such as reef fish (Roberts and Ormond 1987; Gratwicke and Speight 2005; Johnson 2007), providing habitat (Sutton 1985), breeding grounds (Olivotto et al. 2003) and a source of food (Sutton 1985). Such a loss of habitat, breeding grounds and food causes major disturbances in reef fish populations dynamics (Harmelin-Vivien 1994; Wilson et al. 2006; Chabanet et al. 2010) with cyclones even thought to cause short term behavioural changes in reef fish (Woodley et al. 1981).

While branch breakage does lead to a number of negative ecological effects in a coral reef ecosystem, the rubble, which is left as the result of breakage, becomes a highly important carbonate supply for reef growth. In time large piles of rubble can become rigidly bound together and thus stable, this in turn creates new substrate for which coral larvae can settle on and grow (Rasser and Riegl 2002). This process is vital to ensure these valuable coral reef systems can continue to grow. Thus it is clear that it is vital to understand the processes such as bombardment, which lead to both branch breakage and dislodgement of coral colonies, as they have the potential to significantly affect the ecology of not only coral species, but the entire ecosystem that relies on them.

A limitation of the modelling done here was the use of a single, mean substrate strength parameter when, in reality, substrate strength is highly variable (Madin 2005). Due to the computer processing limitations, I was only able to run the analysis using one estimate of substrate strength. Thus I propose that using a range of different reef substrate strength estimates would result in a substantial change in outcomes – higher rates of breakage compared to dislodgement – for most of these growth forms. It is this limitation that explains my primary reasoning for excluding one branching growth form from my analysis. As a logical extension of the ideas presented in Madin (2005), there is a trend in which simple growth forms such as massive corals are unlikely to be dislodged in weak substrates and therefore will continue to grow in these areas. Whereas, more complex growth forms such as branching corals are likely to be dislodged in weaker substrates and will not be able to keep growing in these areas. Thus it is likely that these growth forms will be found in stronger substrates. I consider that complex growth forms are highly likely to suffer from branch breakage due to their structural mechanics.

Given computational limitations that prevented some planned work to be accomplished before this project due date, I have a series of further tasks to do before publishing this work. First, I will be selecting 2-3 more colonies for each of the growth forms over a range of sizes to improve replication and look for colony size trends. Second, I will be examining the effect of colony orientation and material variability of the results. This is particularly important for substrate strength, which is highly variable (Madin 2005). Third, I will be adding thresholds for colony surface damage in the FEA model in order to investigate relative levels of tissue damage spatially on colonies. Fourth, I will be calculating colony shape factors for each colony in order to determine if hydrodynamic dislodgment or bombardment damage is likely to occur first for a range of bombardment projectile masses. And finally, I will be validating FEA results using data I collected from the field at Lizard Island following a direct hit by a category 3 tropical cyclone.

While the results presented here are preliminary, they have highlighted the importance of a rarely considered process, bombardment, for the destruction on coral reefs during hydrodynamic disturbances. With the combination of knowledge from current models and the outcomes presented here, I am able to demonstrate that there are multiple processes and factors that will affect the likelihood of a coral colony suffering from either branch breakage or whole colony dislodgement. This new information that has been brought to light paves the way for continuing research that will enable us to better understand the process of bombardment, has enabled us to more comprehensively understand structural mechanics of coral colonies and has shown that there are multiple processes which can lead to coral damage during a hydrodynamic disturbance. I hope that by increasing our knowledge of both the processes that destroy coral reefs as well as the structural mechanics of different coral morphologies I will be better able to plan, manage and help with the recovery of these vulnerable yet vital ecosystems.

Acknowledgements

I would like to thank Joshua Madin for assistance with experimental analysis; Kyle Zawada for assistance in providing the three-dimensional coral scans; Aaron Harmer and Laura Wilson for assistance with the use of Strand7; Joshua Madin, Rachel Woods and Jessica Thompson for comments on a draft of this manuscript.

References

Autodesk Research (2016) Meshmixer. Autodesk Inc, San Rafael, CA, USA

Bak RP, Criens SR (1981) Survival after fragmentation of colonies of Madracis mirabilis, Acropora palmata and A. cervicornis (Scleractinia) and the subsequent impact of a coral disease. Proceedings of the Fourth International Coral Reef Symposium 2:221-227

Brandt ME, Smith TB, Correa AMS, Vega-Thurber R (2013) Disturbance Driven Colony Fragmentation as a Driver of a Coral Disease Outbreak. Plos ONE 8:e57164

Bruno JF, Selig ER, Casey KS, Page CA, Willis BL, Harvell CD, Sweatman H, Melendy AM (2007) Thermal Stress and Coral Cover as Drivers of Coral Disease Outbreaks. PloS Biology 5:e124

Chabanet P, Guillemot N, Kulbicki M, Vigliola L, Sarramegna Sb (2010) Baseline study of the spatio-temporal patterns of reef fish assemblages prior to a major mining project in New Caledonia (South Pacific). Marine Pollution Bulletin 61:598-611

Chavanich S, Viyakarn V, Sojisuporn P, Siripong A, Menasveta P (2008) Patterns of coral damage associated with the 2004 Indian Ocean tsunami at Mu Ko Similan Marine National Park, Thailand. Journal of Natural History 42:177-187

Connell JH (1978) Diversity in Tropical Rain Forests and Coral Reefs. Science 199:1302-1310

Cooke CA, Marx DE, Jr (2015) Assessment of the Impact of Super Storm Sandy on Coral Reefs of Guantánamo Bay, Cuba. SSC Pacific, San Diego, CA

Creaform (2016a) Exascan Scanner. Creaform, Lévis, Québec

Creaform (2016b) VXElements. Creaform, Lévis, Québec

Fabricius KE, De'ath G, Puotinen ML, Done T, Cooper TF, Burgess SC (2008) Disturbance gradients on inshore and offshore coral reefs caused by a severe tropical cyclone. Limnology and Oceanography 53:690-704

Gratwicke B, Speight MR (2005) The relationship between fish species richness, abundance and habitat complexity in a range of shallow tropical marine habitats. Journal of Fish Biology 66:650-667

Guillemot N, Chabanet P, Pape OL (2010) Cyclone effects on coral reef habitats in New Caledonia (South Pacific). Coral Reefs 29:445-453

Harmelin-Vivien ML (1994) The Effects of Storms and Cyclones on Coral Reefs: A Review. Journal of Coastal Research Special Issue No. 12. COASTAL HAZARDS: PERCEPTION, SUSCEPTIBILITY AND MITIGATION:211-231

Hawkins JP, Roberts CM (1992) Effects of recreational SCUBA diving on fore-reef slope communities of coral reefs. Biological Conservation 62:171-178

Henry L-A, Hart M (2005) Regeneration from Injury and Resource Allocation in Sponges and Corals – a Review. International Review of Hydrobiology 90:125-158

Highsmith RC (1982) Reproduction by Fragmentation in Corals. Marine Ecology Progress Series 7:207-226

Hughes T (2016) The 2016 Coral Bleaching Event in Australia [abstract]. International Coral Reef Symposium; 2016 June 19-24 Session 30

Johnson DW (2007) Habitat Complexity Modifies Post-Settlement Mortality And Recruitment Dynamics Of A Marine Fish. Ecology 88:1716-1725

Katz SM, Pollock FJ, Bourne DG, Willis BL (2014) Crown-of-thorns starfish predation and physical injuries promote brown band disease on corals. Coral Reefs 33:705-716

Knowlton N, Lang JC, Rooney MC, Clifford P (1981) Evidence for delayed mortality in hurricane-damaged Jamaican staghorn corals. Nature 294:251-252

Lirman D (2000) Fragmentation in the branching coral Acropora palmata (Lamarck): growth, survivorship, and reproduction of colonies and fragments. Journal of Experimental Marine Biology and Ecology 251:41-57

Ma C-C, Chuang K-C (2008) Investigation of the transient behavior of a cantilever using a point-wise fiber Bragg grating displacement sensor system. Smart Materials and Structures 17:065010

Madin JS (2005) Mechanical limitations of reef corals during hydrodynamic disturbances. Coral Reefs 24:630-635

Madin JS, Connolly SR (2006) Ecological consequences of major hydrodynamic disturbances on coral reefs. Nature 444:477-480

Madin JS, Black KP, Connolly SR (2006) Scaling water motion on coral reefs: from regional to organismal scales. Coral Reefs 25:635-644

Madin JS, Hoogenboom MO, Connolly SR (2012) Integrating physiological and biomechanical drivers of population growth over environmental gradients on coral reefs. The Journal of Experimental Biology 215:968-976

Madin JS, Baird AH, Dornelas M, Connolly SR (2014) Mechanical vulnerability explains size-dependent mortality of reef corals. Ecology Letters 17:1008-1015

Madin JS, Anderson KD, Andreasen MH, Bridge TCL, Cairns SD, Connolly SR, Darling ES, Diaz M, Falster DS, Franklin EC, Gates RD, Hoogenboom MO, Huang D, Keith SA, Kosnik MA, Kuo C-Y, Lough JM, Lovelock CE, Luiz O, Martinelli J, Mizerek T, Pandolfi JM, Pochon X, Pratchett MS, Putnam HM, Roberts TE, Stat M, Wallace CC, Widman E, Baird AH (2016) The Coral Trait Database, a curated database of trait information for coral species from the global oceans. Scientific Data 3:160017

Mao Y-M, Guo X-L, Zhao Y (2009) Experimental Study of Hammer Impact Identification on a Steel Cantilever Beam. Experimental Techniques 34:82-85

Massel SR, Done TJ (1993) Effects of cyclone waves on massive coral assemblages on the Great Barrier Reef: meteorology, hydrodynamics and demography. Coral Reefs 12:153-166

Olivotto I, Cardinali M, Barbaresi L, Maradonna F, Carnevali O (2003) Coral reef fish breeding: the secrets of each species. Aquaculture 224:69-78

Pateiro-Lopez B, Rodriguez-Casal A (2016) alphahull: Generalization of the Convex Hull of a Sample of Points in the Plane, https://cran.r-project.org/web/packages/alphahull/index.html R package version 2.1

Puotinen M, Maynard JA, Beeden R, Radford B, Williams GJ (2016) A robust operational model for predicting where tropical cyclone waves damage coral reefs. Scientific Reports 6:26009

R Core Team (2014) R: A Language and Environment for Statistical Computing. R Foundation for Statistical Computing, Vienna, Austria

Rasser MW, Riegl B (2002) Holocene coral reef rubble and its binding agents. Coral Reefs 21:57-72

Roberts CM, Ormond RFG (1987) Habitat complexity and coral reef fish diversity and abundance on Red Sea fringing reefs. Marine Ecology Progress Series 41:1-8

Ruiz PD, Kaufmann GH, Möller O, Galizzi GE (2000) Evaluation of impact-induced transient deformations using double-pulsed electronic speckle pattern interferometry and "nite elements. Optics and Lasers in Engineering 32:473-484

Smith LD, Hughes TP (1999) An experimental assessment of survival, re-attachment and fecundity of coral fragments. Journal of Experimental Marine Biology and Ecology 235:147-164

Strand7 Pty Ltd (2015) Strand7 Finite Element Analysis System. Strand7 Sydney, Australia

Sun CT (1977) An Analytical Method for Evaluation of Impact Damage Energy of Laminated Composites Composite Materials: Testing and Design (Fourth Conference). American Society for Testing and Materials 427-440

Sutton M (1985) Patterns of spacing in a coral reef fish in two habitats on the Great Barrier Reef. Animal Behaviour 33:1332-1337

Tunnicliffe V (1981) Breakage and propagation of the stony coral Acropora cervicornis. Proceedings of the National Academy of Sciences of the United States of America 78:2427

Wallace CC (1985) Reproduction, recruitment and fragmentation in nine sympatric species of the coral genus Acropora. Marine Biology 88:217-233

Wilson SK, Graham NAJ, Pratchett MS, Jones GP, Polunin ZVC (2006) Multiple disturbances and the global degradation of coral reefs: are reef fishes at risk or resilient? Global Change Biology 12:2220-2234

Winkler R, Antonius A, Renegar DA (2004) The Skeleton Eroding Band Disease on Coral Reefs of Aqaba, Red Sea. Marine Ecology 25:129-144

Woodley JD, Chornesky EA, Clifford PA, Jackson JBC, Kaufman LS, Knowlton N, Lang JC, Pearson MP, Porter JW, Rooney MC, Rylaarsdam KW, Tunnicliffe VJ, Wahle CM, Wulff JL, Curtis ASG, Dallmeyer MD, Jupp BP, Koehl MAR, Neigel J, Sides EM (1981) Hurricane Allen's Impact on Jamaican Coral Reefs. Science 214:749-755

Youcef-Toumi K, Guts DA (1989) Impact and force control IEEE International Conference on Robotics and Automation. IEEE 410-416

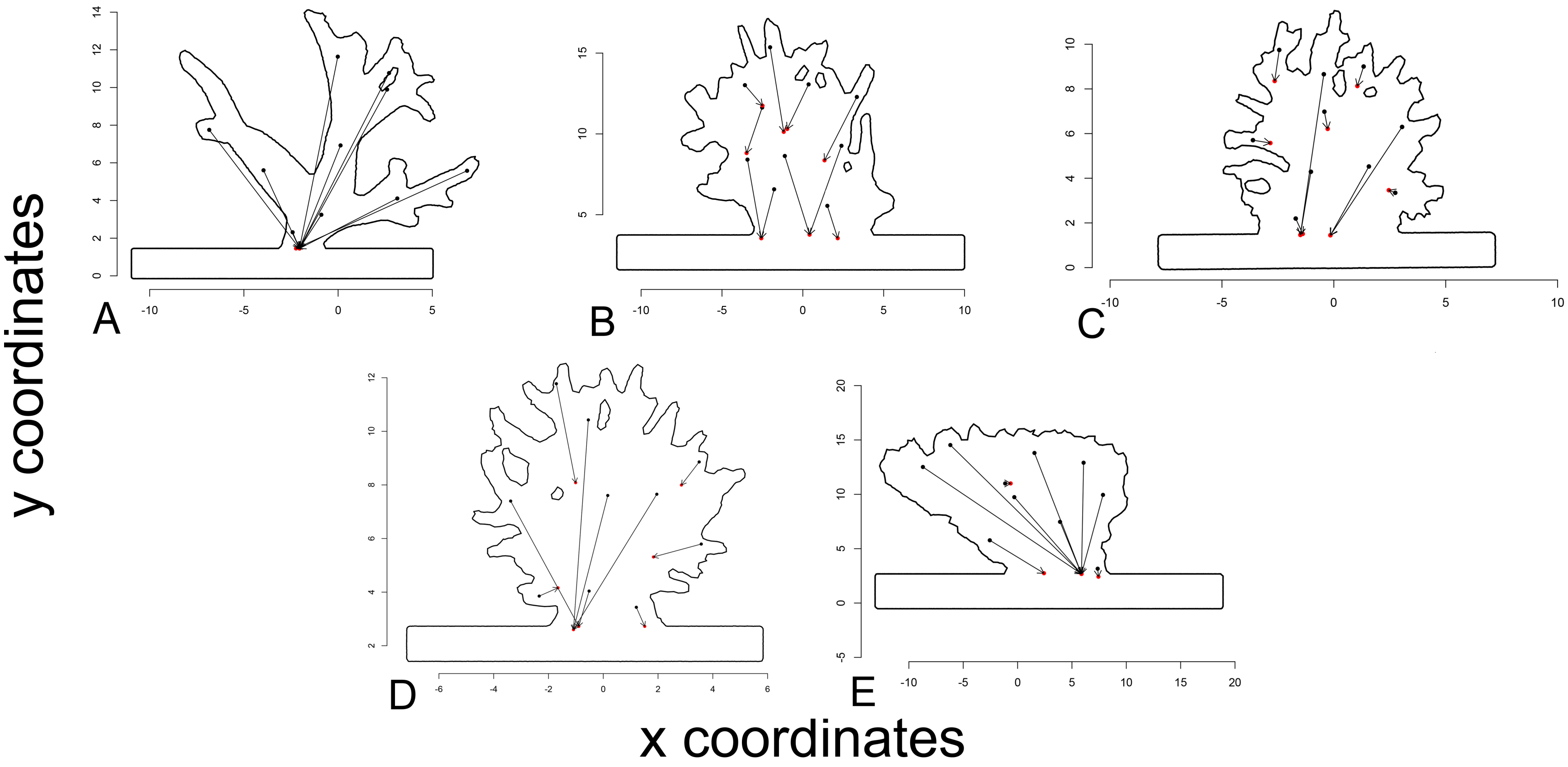

Figure S1.1. Plots modelling the outcome (breakage or dislodgement) of random bombardment impacts from debris for a range of coral growth forms. Black circle: Area of impact, Red circle: Area of breakage/dislodgement. Arrows point from area of impact to area of breakage. Growth forms are as follows: Branching; A, B, Corymbose; C, D, Digitate; E.

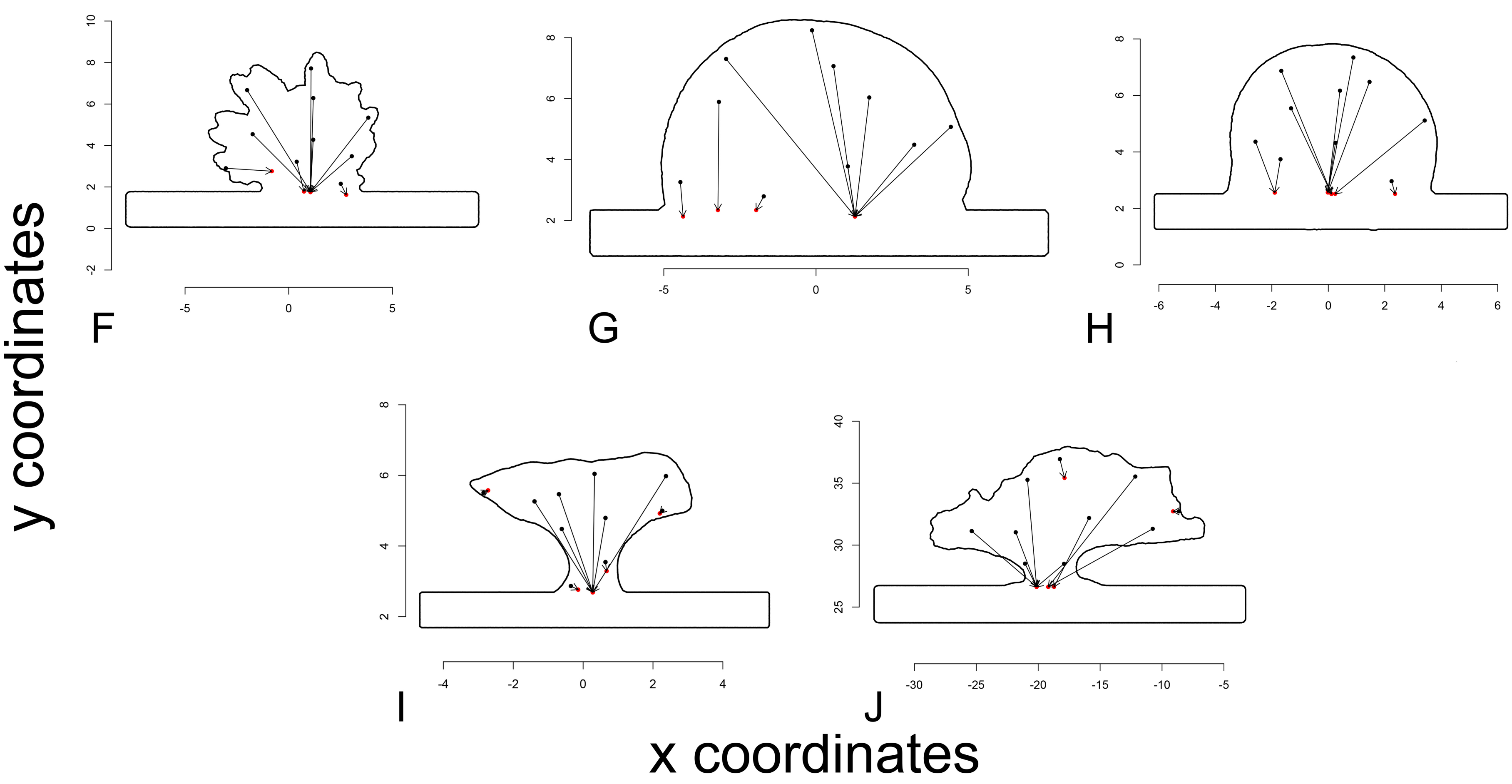

Figure S1.2. Plots modelling the outcome (breakage or dislodgement) of random bombardment impacts from debris for a range of coral growth forms. Black circle: Area of impact, Red circle: Area of breakage/dislodgement. Arrows point from area of impact to area of breakage. Growth forms are as follows: Digitate; F, Massive; G, H and Plating; I, J.

Table S1. Colony impact results and dimensions. Columns are as follows: *id*: colony id, *growth.form*: colony growth form, *brk.dis*: outcome (0: dislodgement, 1: breakage), *imp.force.mpa*: force of impact, *x.cm*: width, *z.cm*: height, *surf.cm2*: surface area (cm^2), *vol.cm3*: volume (cm^3) and *sa.v*: surface area to volume ratio.

id	growth.form	brk.dis	imp.force.mpa	x.cm	y.cm	surf.cm2	vol.cm3	sa.v
31	branch	1	90	12.3	21.4	8279.8	35909.2	0.230576008
31	branch	0	57	12.3	21.4	8279.8	35909.2	0.230576008
31	branch	1	18	12.3	21.4	8279.8	35909.2	0.230576008
31	branch	1	60	12.3	21.4	8279.8	35909.2	0.230576008
31	branch	0	81	12.3	21.4	8279.8	35909.2	0.230576008
31	branch	0	60	12.3	21.4	8279.8	35909.2	0.230576008
31	branch	0	84	12.3	21.4	8279.8	35909.2	0.230576008
31	branch	1	18	12.3	21.4	8279.8	35909.2	0.230576008
31	branch	0	42	12.3	21.4	8279.8	35909.2	0.230576008
31	branch	1	33	12.3	21.4	8279.8	35909.2	0.230576008
33	branch	0	9	15.9	15.2	3142.1	10296.9	0.305150094
33	branch	0	15	15.9	15.2	3142.1	10296.9	0.305150094
33	branch	0	6	15.9	15.2	3142.1	10296.9	0.305150094
33	branch	0	6	15.9	15.2	3142.1	10296.9	0.305150094
33	branch	0	9	15.9	15.2	3142.1	10296.9	0.305150094
33	branch	0	24	15.9	15.2	3142.1	10296.9	0.305150094
33	branch	0	15	15.9	15.2	3142.1	10296.9	0.305150094
33	branch	0	9	15.9	15.2	3142.1	10296.9	0.305150094
33	branch	0	6	15.9	15.2	3142.1	10296.9	0.305150094
33	branch	0	6	15.9	15.2	3142.1	10296.9	0.305150094
59	mass	0	126	7.4	8.6	2080.9	22326	0.093205232
59	mass	0	114	7.4	8.6	2080.9	22326	0.093205232
59	mass	0	288	7.4	8.6	2080.9	22326	0.093205232
59	mass	0	468	7.4	8.6	2080.9	22326	0.093205232
59	mass	0	294	7.4	8.6	2080.9	22326	0.093205232
59	mass	0	480	7.4	8.6	2080.9	22326	0.093205232
59	mass	0	282	7.4	8.6	2080.9	22326	0.093205232
59	mass	0	306	7.4	8.6	2080.9	22326	0.093205232
59	mass	0	282	7.4	8.6	2080.9	22326	0.093205232
59	mass	0	270	7.4	8.6	2080.9	22326	0.093205232
9	mass	0	408	10.2	11.1	3048.5	42890	0.071077174
9	mass	0	258	10.2	11.1	3048.5	42890	0.071077174
9	mass	0	276	10.2	11.1	3048.5	42890	0.071077174
9	mass	0	216	10.2	11.1	3048.5	42890	0.071077174

9	mass	0	144	10.2	11.1	3048.5	42890	0.071077174
9	mass	0	294	10.2	11.1	3048.5	42890	0.071077174
9	mass	0	264	10.2	11.1	3048.5	42890	0.071077174
9	mass	0	240	10.2	11.1	3048.5	42890	0.071077174
9	mass	0	270	10.2	11.1	3048.5	42890	0.071077174
9	mass	0	228	10.2	11.1	3048.5	42890	0.071077174
22	digi	0	30	23.3	28.7	27794.9	215584	0.128928399
22	digi	0	48	23.3	28.7	27794.9	215584	0.128928399
22	digi	1	45	23.3	28.7	27794.9	215584	0.128928399
22	digi	0	57	23.3	28.7	27794.9	215584	0.128928399
22	digi	0	66	23.3	28.7	27794.9	215584	0.128928399
22	digi	0	24	23.3	28.7	27794.9	215584	0.128928399
22	digi	0	57	23.3	28.7	27794.9	215584	0.128928399
22	digi	0	21	23.3	28.7	27794.9	215584	0.128928399
22	digi	0	42	23.3	28.7	27794.9	215584	0.128928399
22	digi	0	39	23.3	28.7	27794.9	215584	0.128928399
24	digi	0	54	8.4	12.2	3944.5	16184.2	0.243725362
24	digi	0	75	8.4	12.2	3944.5	16184.2	0.243725362
24	digi	0	45	8.4	12.2	3944.5	16184.2	0.243725362
24	digi	0	27	8.4	12.2	3944.5	16184.2	0.243725362
24	digi	0	30	8.4	12.2	3944.5	16184.2	0.243725362
24	digi	1	69	8.4	12.2	3944.5	16184.2	0.243725362
24	digi	0	42	8.4	12.2	3944.5	16184.2	0.243725362
24	digi	0	27	8.4	12.2	3944.5	16184.2	0.243725362
24	digi	0	15	8.4	12.2	3944.5	16184.2	0.243725362
24	digi	0	57	8.4	12.2	3944.5	16184.2	0.243725362
12	cory	1	15	10.6	11.8	4843	13852.1	0.349622079
12	cory	0	102	10.6	11.8	4843	13852.1	0.349622079
12	cory	0	72	10.6	11.8	4843	13852.1	0.349622079
12	cory	0	51	10.6	11.8	4843	13852.1	0.349622079
12	cory	1	84	10.6	11.8	4843	13852.1	0.349622079
12	cory	0	72	10.6	11.8	4843	13852.1	0.349622079
12	cory	1	18	10.6	11.8	4843	13852.1	0.349622079
12	cory	0	45	10.6	11.8	4843	13852.1	0.349622079
12	cory	1	27	10.6	11.8	4843	13852.1	0.349622079
12	cory	1	30	10.6	11.8	4843	13852.1	0.349622079
17	cory	0	57	10.3	12.9	4700.6	10372.1	0.453196556
17	cory	0	24	10.3	12.9	4700.6	10372.1	0.453196556
17	cory	0	24	10.3	12.9	4700.6	10372.1	0.453196556
17	cory	1	51	10.3	12.9	4700.6	10372.1	0.453196556
17	cory	0	15	10.3	12.9	4700.6	10372.1	0.453196556
17	cory	1	18	10.3	12.9	4700.6	10372.1	0.453196556
17	cory	0	45	10.3	12.9	4700.6	10372.1	0.453196556

17	cory	0	21	10.3	12.9	4700.6	10372.1	0.453196556
17	cory	1	12	10.3	12.9	4700.6	10372.1	0.453196556
17	cory	1	30	10.3	12.9	4700.6	10372.1	0.453196556
115	plate	1	45	6.4	5.7	929	2148	0.432495345
115	plate	0	72	6.4	5.7	929	2148	0.432495345
115	plate	0	36	6.4	5.7	929	2148	0.432495345
115	plate	1	69	6.4	5.7	929	2148	0.432495345
115	plate	0	19	6.4	5.7	929	2148	0.432495345
115	plate	0	24	6.4	5.7	929	2148	0.432495345
115	plate	0	33	6.4	5.7	929	2148	0.432495345
115	plate	0	27	6.4	5.7	929	2148	0.432495345
115	plate	0	39	6.4	5.7	929	2148	0.432495345
115	plate	1	186	6.4	5.7	929	2148	0.432495345
123	plate	0	36	18.9	22.2	16026.1	49466	0.323982129
123	plate	1	36	18.9	22.2	16026.1	49466	0.323982129
123	plate	0	30	18.9	22.2	16026.1	49466	0.323982129
123	plate	0	27	18.9	22.2	16026.1	49466	0.323982129
123	plate	0	105	18.9	22.2	16026.1	49466	0.323982129
123	plate	0	57	18.9	22.2	16026.1	49466	0.323982129
123	plate	0	48	18.9	22.2	16026.1	49466	0.323982129
123	plate	0	36	18.9	22.2	16026.1	49466	0.323982129
123	plate	0	27	18.9	22.2	16026.1	49466	0.323982129
123	plate	1	63	18.9	22.2	16026.1	49466	0.323982129

Table S2. Detailed outcome results for massive colony, ID 9.

point	imp_str_mpa	imp_brick	imp_node	imp_x	imp_y	imp_z	brk_brick	brk_node	brk_x	brk_y	brk_z
1	408	5902	21238	-3.189192	-3.668323	5.890753	95787	8656	-3.22285	-3.196898	2.338192
2	258	5268	22216	0.574096	-3.668322	7.066781	98859	14883	1.279712	-4.844353	2.127465
3	276	114149	15032	1.044507	-4.609146	3.773904	98859	14883	1.279712	-4.844353	2.127465
4	216	103320	21725	-2.953986	-1.786678	7.301985	98859	14883	1.279712	-4.844353	2.127465
5	144	111989	8138	-1.717357	-3.880629	2.789991	40593	2287	-1.965839	-3.734303	2.338192
6	294	111124	11668	3.227756	-4.598168	4.485281	98859	14883	1.279712	-4.844353	2.127465
7	264	23202	11039	1.749642	-4.659318	6.036568	98859	14883	1.279712	-4.844353	2.127465
8	240	98786	22012	-0.13152	-1.081056	8.242807	98859	14883	1.279712	-4.844353	2.127465
9	270	107334	10392	-4.455688	-2.706289	3.256632	3430	13357	-4.365219	-2.727503	2.127464
10	228	13567	10511	4.42979	-2.987934	5.071235	98859	14883	1.279712	-4.844353	2.127465

For tables S2-S11, columns are as follows: *point*: simulation, *imp_str_mpa*: force of impact, *imp_*brick: impact brick number, *imp_node*: impact bricks central node number, *imp_x, y, z*: central nodes x, y and z coordinates, *brk_brick*: brick number where break occurs, *brk_node*: break bricks central node number, *brk_x, y, z*: central nodes x, y and z coordinates. Nodes can be defined as points placed in a xyz coordinate system that when linked together by elements can form three-dimensional bricks, both elements and bricks may be assigned physical properties such as Young's modulus, Poisson's ratio and density.

Table S3. Detailed outcome results for corymbose colony, ID 12.

point	imp_str_mpa	imp_brick	imp_node	imp_x	imp_y	imp_z	brk_brick	brk_node	brk_x	brk_y	brk_z
1	15	117767	17027	-2.4392	-0.018079	9.744123	176470	42343	-2.643973	0.155611	8.354076
2	102	8610	28999	1.567248	-1.652443	4.526487	117292	40752	-0.152903	-2.91848	1.448023
3	72	9650	25392	-1.02393	-2.830251	4.290931	170346	24802	-1.495054	-2.830262	1.464182
4	51	85317	13600	-1.703372	-2.330366	2.195968	157892	7775	-1.389456	-2.837758	1.509985
5	84	7502	28794	2.745057	-1.652448	3.348676	22256	21208	2.458582	-1.84847	3.46536
6	72	40344	10407	3.050474	-0.503005	6.296984	117292	40752	-0.152903	-2.91848	1.448023
7	18	119554	37587	1.331691	-1.652399	9.002162	32290	13639	1.050805	-2.193102	8.128747
8	45	14212	12536	-0.44737	-2.364658	8.656372	170346	24802	-1.495054	-2.830262	1.464182
9	27	2372	33119	-3.615111	0.46762	5.70428	168529	14117	-2.836617	-0.117831	5.576853
10	30	37114	21534	-0.421394	-3.553472	6.980113	130400	13427	-0.274463	-3.213894	6.210816

Table S4. Detailed outcome results for corymbose colony, ID 17.

point	imp_str_mpa	imp_brick	imp_node	imp_x	imp_y	imp_z	brk_brick	brk_node	brk_x	brk_y	brk_z
1	57	13651	27937	1.207681	-0.842877	3.435072	50503	747	1.51411	-1.424587	2.722049
2	24	10193	38619	-3.380713	-2.510821	7.397677	178115	9045	-0.894333	-1.05739	2.722052
3	24	5642	38823	0.164974	-1.259827	7.60606	158	24331	-1.086313	-0.634339	2.600898
4	51	176028	24440	-2.338681	-1.67586	3.851982	27281	13960	-1.652398	-1.204341	4.160818
5	15	303	1189	-0.544337	0.122574	10.425011	158	24331	-1.086313	-0.634339	2.600898
6	18	5830	40970	3.501857	0.826278	8.857555	41868	1158	2.854153	1.419623	7.996182
7	45	19580	17730	-0.516909	-1.540997	4.039155	178115	9045	-0.894333	-1.05739	2.722052
8	21	33857	7277	1.955206	-0.302198	7.653289	158	24331	-1.086313	-0.634339	2.600898
9	12	8472	39926	-1.712417	2.287163	11.776666	181771	43133	-1.009035	1.534833	8.083841
10	30	26375	15884	3.577966	0.426169	5.793732	15470	37361	1.833437	0.617297	5.311948

Table S5. Detailed outcome results for digitate colony, ID 22.

point	imp_str_mpa	imp_brick	imp_node	imp_x	imp_y	imp_z	brk_brick	brk_node	brk_x	brk_y	brk_z
1	30	6440	43378	-8.709881	-9.035958	12.515204	230748	25701	5.880515	-4.400213	2.679076
2	48	233025	22796	6.072213	-11.264413	12.906844	230748	25701	5.880515	-4.400213	2.679076
3	45	168278	42688	-1.140362	-12.568563	11.001295	203345	42761	-0.636551	-12.567656	11.002345
4	57	187366	5889	7.368601	-1.315728	3.15887	168465	33641	7.438486	-1.971356	2.422463
5	66	136059	24933	-2.557997	-3.592074	5.773536	159266	14784	2.426896	-5.579492	2.7432
6	24	10461	43510	-6.186646	-4.998972	14.533704	230748	25701	5.880515	-4.400213	2.679076
7	57	35614	21676	-0.302411	-9.968274	9.740288	230748	25701	5.880515	-4.400213	2.679076
8	21	38384	12067	1.553573	-12.159994	13.804585	230748	25701	5.880515	-4.400213	2.679076
9	42	180579	33707	3.906046	-7.522301	7.468806	230748	25701	5.880515	-4.400213	2.679076
10	39	182672	7988	7.85793	-9.261433	9.94891	230748	25701	5.880515	-4.400213	2.679076

Table S6. Detailed outcome results for digitate colony, ID 24.

point	imp_str_mpa	imp_brick	imp_node	imp_x	imp_y	imp_z	brk_brick	brk_node	brk_x	brk_y	brk_z
1	54	147907	31203	2.508904	-3.823954	2.154316	1416	29646	2.774532	-4.355213	1.623059
2	75	196692	26115	0.383882	-5.152084	3.216835	25003	2118	0.736228	-4.243441	1.782014
3	45	4972	42335	-1.741138	-4.62082	4.544972	139480	31165	1.047952	-3.691141	1.755874
4	27	182597	13111	1.184548	-2.330947	6.2851	139480	31165	1.047952	-3.691141	1.755874
5	30	147226	43251	3.837045	-0.370773	5.34183	139480	31165	1.047952	-3.691141	1.755874
6	69	182886	7735	-3.032927	-3.518619	2.90376	179233	14647	-0.815959	-2.719074	2.761632
7	42	3440	29938	1.180766	-4.886451	4.279345	139480	31165	1.047952	-3.691141	1.755874
8	27	1918	42773	-2.006811	0.160651	6.669986	139480	31165	1.047952	-3.691141	1.755874
9	15	179733	16413	1.076069	-0.436116	7.714137	139480	31165	1.047952	-3.691141	1.755874
10	57	8014	29965	3.040158	-5.152086	3.482461	139480	31165	1.047952	-3.691141	1.755874

Table S7. Detailed outcome results for branching colony, ID 31.

point	imp_str_mpa	imp_brick	imp_node	imp_x	imp_y	imp_z	brk_brick	brk_node	brk_x	brk_y	brk_z
1	90	61033	10191	3.34138	-7.9046	12.285987	78100	18409	1.341784	-5.295778	8.364708
2	57	175397	15947	2.388358	-6.010231	9.265924	138752	7369	0.415096	-0.989272	3.768469
3	18	158205	44512	-2.02345	-3.323762	15.359505	71602	10184	-1.180811	-3.262231	10.12739
4	60	145400	4756	-2.513739	-8.949044	11.632852	958	37553	-3.477039	3.217005	8.816584
5	81	127922	14247	-3.422521	1.774026	8.409944	202910	29477	-2.568337	-1.32652	3.54614
6	60	7572	29069	-1.114552	-6.778611	8.634918	138752	7369	0.415096	-0.989272	3.768469
7	84	178623	17583	1.516482	-1.675553	5.550084	3782	40678	2.156894	0.490876	3.546138
8	18	170741	15029	0.35715	-5.797732	13.064109	161978	10279	-0.964605	-6.326497	10.304526
9	42	67603	6693	-1.774249	0.729746	6.573741	202910	29477	-2.568337	-1.32652	3.54614
10	33	77971	11565	-3.580653	-8.674071	13.015917	73250	11761	-2.492456	-8.55803	11.74828

Table S8. Detailed outcome results for branching colony, ID 33.

point	imp_str_mpa	imp_brick	imp_node	imp_x	imp_y	imp_z	brk_brick	brk_node	brk_x	brk_y	brk_z
1	9	125057	15410	6.844672	-3.386742	5.579333	94798	57	-2.2349	-1.825966	1.454844
2	15	127287	27045	3.14103	-1.638283	4.108542	94659	5369	-2.048005	-1.690758	1.454859
3	6	114444	18788	2.703884	0.893741	10.766365	94659	5369	-2.048005	-1.690758	1.454859
4	6	11711	16866	-6.839264	0.69332	7.750384	94659	5369	-2.048005	-1.690758	1.454859
5	9	11441	19717	-3.958373	-2.119833	5.60491	94659	5369	-2.048005	-1.690758	1.454859
6	24	120806	1088	-2.413152	-1.643009	2.314442	94585	5369	-2.048005	-1.690758	1.454859
7	15	1263	26346	-0.889321	-2.50224	3.244917	94659	5369	-2.048005	-1.690758	1.454859
8	9	133979	20598	0.129431	-1.156183	6.924761	94659	5369	-2.048005	-1.690758	1.454859
9	6	12696	15990	-0.017017	2.51057	11.637128	94659	5369	-2.048005	-1.690758	1.454859
10	6	123753	19013	2.599939	1.964352	9.892537	94659	5369	-2.048005	-1.690758	1.454859

Table S9. Detailed outcome results for massive colony, ID 59.

point	imp_str_mpa	imp_brick	imp_node	imp_x	imp_y	imp_z	brk_brick	brk_node	brk_x	brk_y	brk_z
1	126	6704	28593	2.241155	-2.802158	2.964065	186544	3996	2.365096	-3.061548	2.515309
2	114	174849	41203	-1.665136	-1.630256	6.870356	180509	6952	0.111133	-4.237122	2.515309
3	288	152761	17541	0.253074	-4.061909	4.321778	180640	11519	-0.015606	-4.179635	2.565516
4	468	174286	42217	1.459897	-2.606844	6.479726	180640	11519	-0.015606	-4.179635	2.565516
5	294	205114	3646	-2.579395	-3.101306	4.362473	183329	335	-1.895738	-3.79414	2.561041
6	480	3765	42604	3.413041	-1.23964	5.112525	98551	5692	0.242533	-4.274228	2.515309
7	282	25116	11147	0.413376	-3.401146	6.169199	180640	11519	-0.015606	-4.179635	2.565516
8	306	183812	4861	-1.694044	-3.802557	3.740809	183329	335	-1.895738	-3.79414	2.561041
9	282	183971	5593	-1.31951	-3.597834	5.54402	180509	6952	0.111133	-4.237122	2.515309
10	270	132353	10752	0.887756	-1.777325	7.343683	180640	11519	-0.015606	-4.179635	2.565516

Table S10. Detailed outcome results for plating colony, ID 115.

point	imp_str_mpa	imp_brick	imp_node	imp_x	imp_y	imp_z	brk_brick	brk_node	brk_x	brk_y	brk_z
1	45	10798	11883	-2.849734	-1.361147	5.507936	49702	20256	-2.719654	-1.443228	5.575875
2	72	91966	20423	-1.391105	-1.757613	5.26295	62648	6368	0.276158	-1.428904	2.689113
3	36	5410	20564	-0.609843	-0.820111	4.481671	62648	6368	0.276158	-1.428904	2.689113
4	69	7344	15724	0.640177	-0.351401	3.544151	13280	10380	0.672989	-0.812121	3.291179
5	19	78280	21507	0.327681	2.304971	6.044087	62648	6368	0.276158	-1.428904	2.689113
6	24	87745	4794	2.371861	0.136417	5.980114	62648	6368	0.276158	-1.428904	2.689113
7	33	13819	10834	-0.34966	-0.947758	2.866344	79614	13992	-0.141087	-0.976373	2.7629
8	27	77432	20743	0.640194	-1.91386	4.794211	62648	6368	0.276158	-1.428904	2.689113
9	39	10391	9224	-0.6916	1.207097	5.467509	62648	6368	0.276158	-1.428904	2.689113
10	186	20694	9390	2.267306	-2.144835	4.997812	20696	9387	2.19559	-2.240448	4.922196

Table S11. Detailed outcome results for plating colony, ID 123.

point	imp_str_mpa	imp_brick	imp_node	imp_x	imp_y	imp_z	brk_brick	brk_node	brk_x	brk_y	brk_z
1	36	19563	10507	-25.371085	32.455927	31.136614	127255	25260	-20.126761	34.210794	26.62962
2	36	4412	36325	-18.25136	34.211606	36.942442	157256	38913	-17.872341	34.357205	35.423277
3	30	146228	17826	-20.866282	35.330505	35.271994	127255	25260	-20.126761	34.210794	26.62962
4	27	27229	11829	-21.816974	30.989359	31.037972	127255	25260	-20.126761	34.210794	26.62962
5	105	146714	15395	-17.914412	35.272849	28.492964	127255	25260	-20.126761	34.210794	26.62962
6	57	4144	25549	-21.064274	35.617085	28.504643	127255	25260	-20.126761	34.210794	26.62962
7	48	5808	14246	-15.892443	27.914636	32.18955	73385	25321	-18.720485	35.148307	26.629623
8	36	490	36780	-10.751558	34.679947	31.317254	82159	25290	-19.189237	34.679551	26.629629
9	27	119537	37033	-12.157802	36.555348	35.536045	82159	25290	-19.189237	34.679551	26.629629
10	63	7118	37051	-8.642163	31.867227	32.72356	6777	37093	-9.110379	32.339808	32.726167